Available online at www.sciencedirect.com
ScienceDirect
Bioelectrochemistry 72 (2008) 174–182
Bioelectrochemistry
www.elsevier.com/locate/bioelechem

Scanning electrochemical microscopy study of laccase within a sol–gel processed silicate film

Wojciech Nogala [a], Malte Burchardt [b], Marcin Opallo [a,*], Jerzy Rogalski [c], Gunther Wittstock [b,*]

[a] *Institute of Physical Chemistry, Polish Academy of Sciences, ul. Kasprzaka 44/52, PL-01-224 Warszawa, Poland*
[b] *Carl von Ossietzky University of Oldenburg, Faculty of Mathematics and Science, Center of Interface Science (CIS), Department of Pure and Applied Chemistry and Institute for Chemistry and Biology of the Marine Environment, D-26111 Oldenburg, Germany*
[c] *Maria Curie Sklodowska University, Department of Biochemistry, Pl. Marii Curie Skodowskiej 3, PL-20-031 Lublin, Poland*

Received 8 January 2008; received in revised form 18 January 2008; accepted 31 January 2008
Available online 16 February 2008

Abstract

The enzyme *p*-diphenol:dioxygen oxidoreductase (laccase, EC 1.10.3.2) was isolated from *Cerrena unicolor* fungus and embedded in a sol–gel film obtained by acidic condensation of TMOS. The gel was cast to thin films on glass. The laccase-containing silicate films were inspected by confocal laser scanning microscopy (CLSM), scanning force microscopy (SFM) and scanning electrochemical microscopy (SECM). CLSM images in the reflection mode showed aggregates within the silicate films. SECM images in the substrate-generation/tip-collection mode using 2,2'-azino-bis(3-ethylbenzothiazoline-6-sulfonate) (ABTS) as electron donor for laccase showed that the position of aggregates coincides with increased enzymatic activity within the silicate film. The flux from individual aggregates was detected. SECM images in the redox competition mode confirmed the assignment and could exclude that topographic features observed by CLSM and SFM could be the reason for the image contrast. SFM images showed that the aggregates partially dissolve during prolonged exposure to aqueous buffer. The experimental setup allowed following one individual aggregate over time with all three microscopic techniques which enabled the collection of complementing information on morphology and catalytic activity as well as their development over time.

Keywords: Laccase; Sol–gel; Dioxygen reduction; Scanning electrochemical microscopy (SECM); Scanning force microscopy (SFM); Confocal laser scanning microscopy (CLSM)

1. Introduction

Laccases (*p*-diphenol:dioxygen oxidoreductases, EC 1.10.3.2) belong to the larger group of multicopper enzymes. They are produced by plants, fungi, some bacteria and insects [1–3]. The active site of most of the fungal laccases (i.e. blue oxidase) contains four copper ions in the 2+ oxidation state. One of the most important properties of laccases is its capability to oxidise numerous organic substrates and to reduce dioxygen directly to water without formation of reactive intermediates [3]. These phenomena can be utilised in electrochemical devices if an efficient electron transfer path between the protein and the electrode is provided. Recently, the successful application of laccase-modified electrodes was reported for the oxidation of phenolic substrates [4–6], electrochemical sensing [6–9] and electrocatalytic dioxygen reduction [4–24]. The last system can potentially be applied in biofuel cells [25–28 and refs. cited therein].

For all these applications the stable immobilisation of intact laccase plays a crucial role in the construction of enzyme electrodes. Among others, the use of sol–gel technology seems to be promising. The protein encapsulation into a sol–gel processed silicate matrix preserves its activity and prevents its

* Corresponding authors. Gunther Wittstock is to be contacted at Tel.: +49 441 798 3971; fax: +49 441 798 3979. Marcin Opallo, Tel.: +48 22 343 3375; fax: +48 22 343 3333.
E-mail addresses: mopallo@ichf.edu.pl (M. Opallo), gunther.wittstock@uni-oldenburg.de (G. Wittstock).

1567-5394/$ - see front matter © 2008 Elsevier B.V. All rights reserved.
doi:10.1016/j.bioelechem.2008.01.010

leaching to the surrounding solution [29,30]. Not surprisingly, the sol–gel process has already been applied successfully for the immobilisation of laccase on the electrode surface [8,14,15,18,20–24] and efficient electron exchange between electrode and embedded enzyme was demonstrated. The porous hydrophilic silicate film allows fast diffusion of the redox mediator between the immobilised protein and the electrode. The encapsulation of laccase in silicate matrix has not been restricted to electrochemical devices but was also used in an optical sensor [31].

Among other factors the distribution of laccase immobilised in a silicate matrix and the specific laccase activity affect the efficiency of the resulting electrochemical devices stimulating an interest in local characterisation of such electrodes. Scanning electrochemical microscopy (SECM, [32–34]) has already been widely used to monitor distribution and activity of enzymes immobilised on flat surfaces, e.g. on electrodes and within thin films [35–39]. A number of schemes can be used to monitor the activity of oxygen-reducing enzymes. If H_2O_2 is formed, this compound can be detected in the substrate-generation/tip-collection (SG/TC) mode [38]. If a quantification shall be attempted the modified regions must be a microstructure by itself, in order to form a steady state diffusion layer. The four electron reduction favourable for biofuel cells is more difficult to detect, since the reaction product H_2O is the solvent. If the enzyme is connected to an electrode and an efficient electron transfer is possible, one may use the tip-generation/substrate collection (TG/SC) mode in an oxygen-free solution and use the UME to produce dioxygen by water electrolysis. The locally available dioxygen is then consumed by the enzyme-modified electrode [40]. Plotting the sample current vs. the UME position provides a reactivity image that has been used to screen immobilisation procedures for bilirubin oxidase (BOD) and laccase [40]. One of the drawbacks of this arrangement is the potentially high background currents due to the reduction of dioxygen traces at a macroscopic sample independent of the UME position. The additional contribution from the locally increased oxygen availability has to be determined on this background. Furthermore, the sample has to be an electrode because otherwise the substrate conversion cannot be measured. These problems have been circumvented by the redox competition (RC) mode. In this mode, active areas on the sample and the microelectrode compete for dissolved dioxygen [41]. Catalytically active areas on the sample are identified by reduced oxygen-reduction currents at the UME. The sensitivity can be enhanced by applying a pulse programme to the UME. In a prepulse the UME is used to produce dioxygen by water electrolysis in order to supersaturate the solution between the UME and the sample. In the detection pulse, dissolved dioxygen is reduced at the UME and the detected amount is decreased if the sample is also consuming dioxygen [42]. This concept has been applied to BOD wired to a redox polymer [41].

This paper presents investigations of laccase distribution within sol–gel processed silicate films by SECM. A glass plate was used as support because of its flat surface, strong affinity to silicate films and insulating character. The SECM investigations are performed with 2,2'-azino-bis(3-ethylbenzothiazoline-6-sulfonate) ($ABTS^{2-}$) as one-electron donor for the laccase-catalysed reduction of dioxygen (Eq. (1)).

$$O_2 + 4\,H^+ + 4\,ABTS^{2-} \rightarrow 2\,H_2O + 4\,ABTS^{\bullet -} \quad (1)$$

The measurements are performed in the SG/TC mode and the RC mode detecting amperometrically either $ABTS^{\bullet -}$ or $ABTS^{2-}$ at the ultramicroelectrode (UME) scanned over the laccase film.

2. Experimental

Laccase was obtained from the *Cerrena unicolor* fungus according to a literature procedure [43,44]. This protein was purified by ion exchange chromatography on DEAE Sepharose (fast flow, Pharmacia, Uppsala, Sweden) connected into ECONO-System chromatograph (Bio-Rad, Herkules, CA, USA) and concentrated on a Pellicon 2 ultrafiltration semiprep cell (10 kDa cut off, Millipore, Billerica, MA, USA). Then laccase was distributed into lyophilisation vials and lyophilised in Labconco FreeZone 12 (Labconco, Kansas, MO, USA). Each vial contained 1.4 mg of protein and 3×10^6 nM s^{-1} of laccase. The activity of the laccase was determined by following the oxidation of 0.025 mM syringaldazine (Sigma-Aldrich, Steinheim, Germany) in 0.1 M citrate–phosphate buffer at pH 5.0 [45] by kinetic measurement at $\lambda = 525$ nm ($\varepsilon_{525} = 6.5\times10^4$ M^{-1} cm^{-1} at 25 °C). The protein content was determined with bovine albumin (Sigma, St. Louis, MO, USA) as a standard [46].

The hydrophilic sol–gel matrix for immobilisation of laccase was prepared by mixing tetramethoxysilane (TMOS, Sigma-Aldrich, Steinheim, Germany), H_2O and 0.04 mol L^{-1} aqueous HCl in volume ratio 18:4.5:1 [18,23]. This mixture was sonicated for 20 min. After mixing with water in volume ratio 1:1, the sol was sonicated for 3 min, diluted with water in 1:100 volume ratio and sonicated for another 3 min. Finally, 145 μg of laccase was added to 250 μL of this solution. 10 μL of the laccase–sol was placed on an area of 0.5 cm^2 on a glass surface. For sol–gel processing and drying these samples were left for at least 20 h at room temperature.

SECM experiments were carried out on two homebuilt SECM [47,48]. The first setup consists of three closed-loop piezo actuators (PI HERA, P625.1CD piezos and LVPZT Amplifier E-509 C3A, PhysikInstrumente, Karlsruhe, Germany) mounted on an inverted optical microscope (Eclipse TS100, Nikon, Düsseldorf, Germany) and an analogue potentiostat (μP3, M. Schramm, Heinrich Heine University of Düsseldorf, Germany). The maximum scan range is 500 μm × 500 μm × 500 μm with a resolution better than 1 nm. The motors and the potentiostat are interfaced via AD/DA cards (PCI-DDA8 and PCI-DAS1602/16, Plug-in Electronic GmbH, Eichenau, Germany). The second SECM mounted on a confocal laser scanning microscope (Leica TCS SP AOBS, Leica Microsystems GmbH, Wetzlar, Germany) uses closed-loop piezo motors (mechOnics AG, München, Germany), controlled via USB interface and a microprocessor controller and a digital potentiostat (CompactStat, Ivium Technologies, Eindhoven, Netherlands). Maximum scan range is

17 mm × 17 mm × 17 mm with a nominal resolution of 50 nm. Both instruments run on the homebuilt software SECMx [47]. Data analysis was performed with the in house package MIRA [49].

SECM measurements were performed in a three electrode cell consisting of a Pt UME as working electrode, a Pt wire as auxiliary electrode and a silver wire as quasi-reference electrode to which all potentials are referred. The UME was obtained by sealing a Pt wire (10 μm diameter, Goodfellow GmbH, Bad Nauheim, Germany) into borosilicate glass capillaries (Hilgenberg GmbH, Malsfeld, Gemany) and shaping the apex according to Kranz et al. [50]. The ratio *RG* between the radius of the insulating glass and the radius r_T of the active electrode area was approximately 9. The sample was mounted and 1 mM $ABTS^{2-}$ in 0.1 M phosphate buffer (pH 4.8, dearated) was used as working solution. Ar was passed over the cell. After assembling all parts, oxygen from air was allowed to diffuse into the electrolyte which started the reaction at the laccase. Oxidation of $ABTS^{2-}$ was carried out at +0.4 V (RC mode), reduction of $ABTS^{\bullet-}$ at −0.1 V (GC mode). Horizontal and vertical translation rates v_T were 4–15 μm s^{-1} and 0.6–3 μm s^{-1}, respectively.

AFM micrographs were recorded at ambient conditions in Tapping Mode™ with a RTESP probe (Veeco, Mannheim, Germany) using a Nanoscope IIIA controller and a Dimension 3100 sample stage (Veeco Instruments Inc., Santa Barbara, CA, USA).

Optical micrographs were obtained by CSLM TCS SP2 AOBS (Leica Microsystems GmbH, Wetzlar, Germany) built as an inverted optical microscope in the reflection mode at a wavelength of 488 nm with a HC PL FLUOTAR 10× objective (numerical aperture NA = 0.3, Leica) and a HC PL FLUOTAR 50× objective (numerical aperture NA = 0.80, Leica).

3. Results and discussion

The investigation of thin films of laccase immobilised in sol–gel matrices using optical microscopy or CLSM (Fig. 1A) reveals features that are considered to be aggregates of laccase. In order to confirm this assignment, combined SECM/CLSM experiments were performed that correlated the optically detectable features in the laccase/silicate film to electrochemical signals (Fig. 1). Several spots are visible in the CLSM image recorded in the reflection mode (Fig. 1A). The inverted setup of the optical microscope allowed to observe the sample during SECM imaging. This feature was used to position the UME of the SECM close to the features of interest by means of optical observation. The UME is visible at the starting point of the experiment as a white spot at the bottom right corner of Fig. 1A. With the help of the motorised and digital stage of the CLSM the UME to sample distance *d* was adjusted to $d \approx 4\, r_T = 20$ μm. The image frame corresponds to the bright region in the optical image in Fig. 1A.

The SECM experiments were carried out in the SG/TC mode (Fig. 1B). A solution of $ABTS^{2-}$ in phosphate buffer was used. $ABTS^{2-}$ serves as the electron donor in the enzymatically driven reduction of dioxygen (Eq. (1)). The reaction product, $ABTS^{\bullet-}$, diffuses into the solution and forms a diffusion layer. At the UME a potential is applied that is sufficiently negative to reduce $ABTS^{\bullet-}$ so that the reaction proceeds according to Eq. (2)

$$ABTS^{\bullet-} + e^- \rightarrow ABTS^{2-} \quad (2)$$

ABTS was selected as electron donor, because of its good solubility in water, its ability to diffuse through the silicate film and efficiently exchange electrons with the prosthetic group of laccase. The insulating nature of the glass support eliminates positive feedback contribution in SG/TC experiment.

When the UME scans across the surface, an increased reduction current i_T is observed at the UME (Fig. 1C) when it is scanned across the features visible in the CLSM image Fig. 1A. A rising background is observed in Fig. 1C because the macroscopic silicate film contains laccase also in areas outside the optically visible aggregates. After allowing the influx of dioxygen into the previously dearated solution from air after assembly and positioning the electrode, the macroscopic laccase–silicate film provides an increasing flux of $ABTS^{\bullet-}$ leading to a steadily increasing bulk concentration. Oxygen from air had to be excluded from the cell during assembly because otherwise the solution composition ($ABTS^{2-}$ consumption) would change too rapidly for recording reasonable images. In order to highlight the signals from the *additional* flux above the laccase aggregates on the rising background, the colour scale (but *not* the vertical position of the datapoints) was corrected by subtracting a second order polynomial (Fig. 1C and E).

A control experiment was performed in order to exclude that topographic features lead to variations of i_T in Fig. 1C and are wrongly interpreted as enzymatic activity. In the SG/TC mode experiment an increased reduction current is also expected if small amounts of $ABTS^{\bullet-}$ are present in the bulk solution and *d* is increased for instance when scanning over a depression in the silicate film. In this case an enhanced diffusional mass transport of $ABTS^{\bullet-}$ to the UME would take place because the shielding of sample and insulating sheath of the UME is reduced at larger *d*. For the control experiment, a potential was applied to the UME in the same working solution at which diffusion-controlled oxidation of $ABTS^{2-}$ takes place. Due to the consumption $ABTS^{2-}$ by the enzymatic reaction at the sample, a decrease of i_T is expected if the UME is scanned over an area with increased laccase activity (Fig. 1D). Compared to the RC mode procedure by Eckhard et al. [42], no pulse programme has been used here. However, for a qualitative detection of enzyme activity the sensitivity was sufficient here in order to detect an additional contribution of the laccase aggregates (Fig. 1E). It even seems that the noise is significantly lower if no potential pulses are applied to the UME. Possible topographic features of the silicate film would lead to the same signal variations as in the SG/TC mode: an increase of *d* leads to an increase of the oxidation current at the UME. The opposite trend is observed in Fig. 1E: the reduced oxidation current above the enzyme

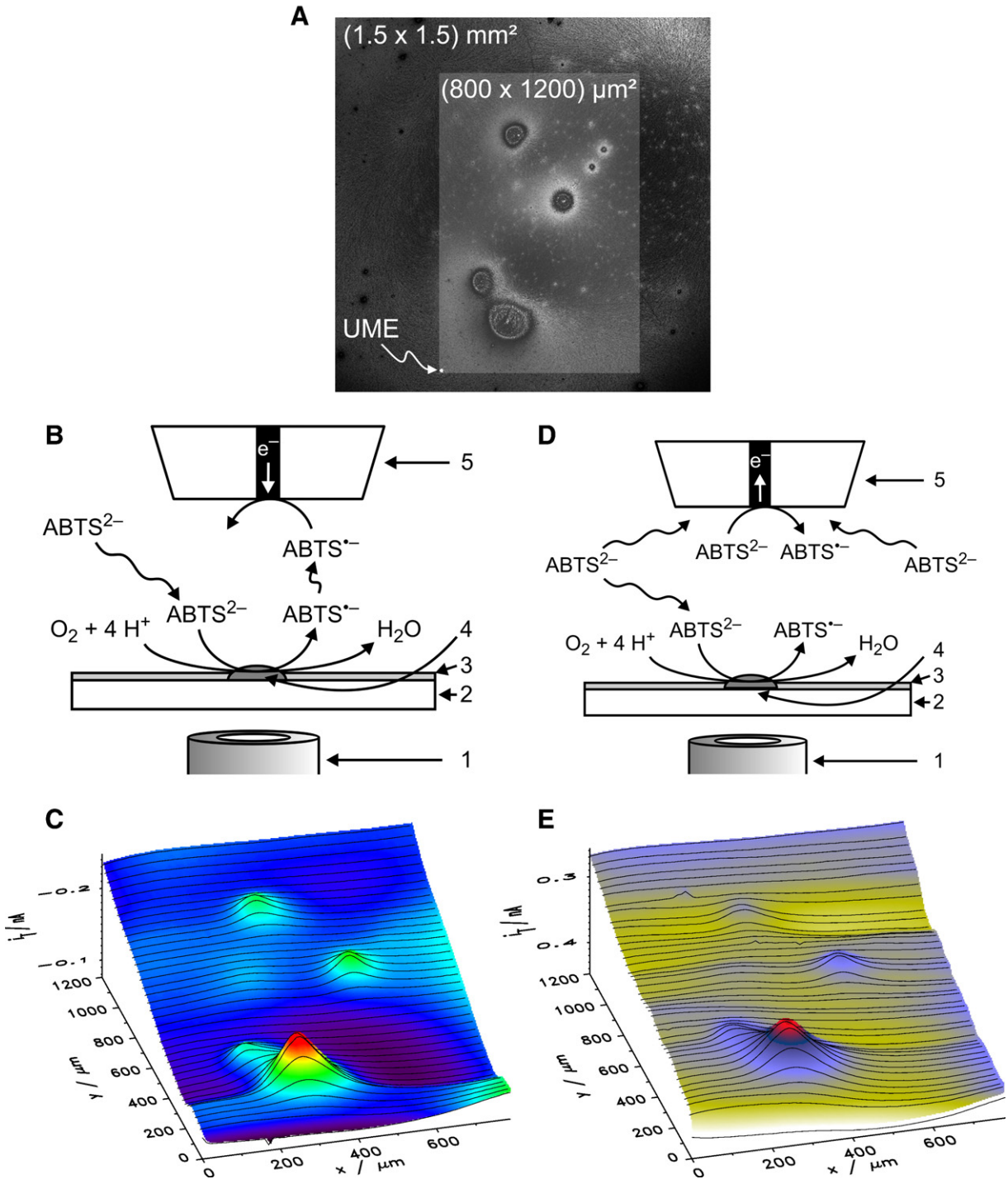

Fig. 1. Combined SECM/CLSM mapping of laccase aggregates. A) Reflection mode CLSM image (10× objective); B) schematic of SG/TC mode SECM imaging of laccase activity (not in scale) 1) microscope objective; 2) glass slide; 3) laccase–silicate film; 4) laccase aggregate; 5) UME; C) SG/TC mode SECM image; E_T= −0.1 V, r_T=5 µm, 1 mM $ABTS^{2-}$+0.1 M phosphate buffer (pH 4.8), v_T=7.7 µm s^{-1}; D) schematic of RC mode SECM imaging of laccase activity (not in scale); E) RC mode SECM image, E_T=+0.4 V, other conditions as in C. Current scales in C and E are inverted to show high activity as "hills".

aggregate indicates the consumption of $ABTS^{2-}$ by the enzymatic reaction. This observation is supported by AFM micrographs (vide infra) and CLSM surface reconstructions (supporting information). In those topographic data, only small features are observed that cannot be responsible for the signals in the SG/TC mode or RC mode experiments at the given $d=4r_T$ where topographic effects do not play an important role.

For quantification of the additional flux from the laccase aggregate, a cross section above the centre of the spot has been

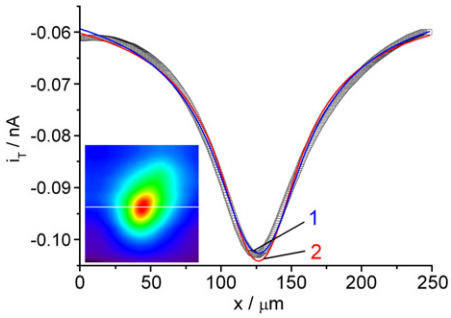

Fig. 2. Flux of $ABTS^{\bullet-}$ produced by individual laccase aggregates. Flux values are obtained from the extracted profile along the white line in the inset and fits to Eqs. (3, 4); symbols — experimental data, curve 1) — fitted curve using $4Dr_Tc_S = 1.583\times10^{-15}$ mol s^{-1}, $x_0 = 126.92$ µm, $d = 23.31$ µm, $r_S = 14.54$ µm, $i_{offset} = 0.0484$ nA, curve 2) fitted result using $4Dr_Tc_S = 1.4631\times10^{-15}$ mol s^{-1}, $x_0 = 126.80$ µm, $d = 20$ µm, $r_S = 13.5$ µm, $i_{offset} = 0.0508$ nA (d and r_S fixed); Experimental parameters: scan area 250 µm × 250 µm, $E_T = -0.1$ V, $r_T = 5$ µm, 1 mM $ABTS^{2-}$ + 0.1 M phosphate buffer (pH 4.8), $v_T = 4.2$ µm s^{-1}.

extracted from a SECM image (Fig. 2). The resulting profile has been fitted to Eqs. (3,4)

$$i_T = 4nFD(ABTS^{\bullet-})r_T[ABTS^{\bullet-}]_S\,\zeta \tag{3}$$

$$\zeta = \frac{2}{\pi}\arctan\frac{\sqrt{2}r_s}{\left(\sqrt{\left(\Delta x^2 + d^2 - r_s^2\right) + \sqrt{\left(\Delta x^2 + d^2 - r_s^2\right)^2 + 4d^2r_s^2}}\right)} \tag{4}$$

that have been developed for diffusion at an isolated disk-shaped pore [51,52], where $n = 1$ is the number of transferred electrons from the UME per $ABTS^{\bullet-}$ molecule, $D(ABTS^{\bullet-}) = 3.2\times10^{-6}$ cm^2 s^{-1} [19] is the diffusion coefficient of $ABTS^{\bullet-}$, $r_T = 5$ µm is the UME radius, r_S is the radius of the enzyme aggregate, $[ABTS^{\bullet-}]_S$ is the increased concentration of $ABTS^{\bullet-}$ at the enzyme aggregate surface, and ζ is a dimensionless factor describing the decrease of the $ABTS^{\bullet-}$ concentration as a function of the lateral distance $\Delta x = x - x_0$ and the vertical distance d from the centre of the spot at (x_0, $d = 0$). Non-linear curve fitting yielded the following adjustable parameters: $4Dr_Tc_S = 1.583\times10^{-15}$ mol s^{-1}, $x_0 = 126.92$ µm, $d = 23.31$ µm, $r_S = 14.54$ µm, $i_{offset} = 0.0484$ nA (Fig. 2B, curve 1).

The fitted value of $d = 23.3$ µm agrees well with the working distance retracted from the surface, checked through an inverted optical microscope, and compared to an approach procedure over glass. The fitted $r_S = 14.5$ µm is consistent with the optical microscopic observation that yielded $r_S = 13.5$ µm. The small offset current is a consequence of the slowly increasing bulk concentration of $ABTS^{\bullet-}$. Fitting of the profile by fixing the parameters d and r_S to the independently determined values leads to results deviating less than 10% from the results of the other fitting strategy ($4Dr_Tc_S = 1.4631\times10^{-15}$ mol s^{-1}, $x_0 = 126.80$ µm, $i_{offset} = 0.0508$ nA; Fig. 2B, curve 2). Therefore, derived values will be reported only for the fit with adjustable r_S and d because the derived values are also within a 10% uncertainty interval. The additional surface concentration $[ABTS^{\bullet-}]_S$ can be estimated to be 9.8×10^{-4} M. From this value, the flux Ω of $ABTS^{\bullet-}$ from the enzyme aggregate can be calculated according to Eq. (5) [52].

$$\Omega = 4D(ABTS^{\bullet-})r_S[ABTS^{\bullet-}]_S = 1.7\times10^{-14}\,\mathrm{mol\,s^{-1}}. \tag{5}$$

Assuming a uniform flux over the enzyme aggregate a generation rate J can be determined according to Eq. (6).

$$J = \Omega/\left(\pi r_S^2\right) = 3.0\times10^{-9}\,\mathrm{mol\,s^{-1}\,cm^{-2}}. \tag{6}$$

This value is 38 times higher than the *average* flux determined from the current density of 0.03 mA cm^{-2} measured at a silicate–laccase-modified ITO electrode with ABTS dissolved in solution [24].

To further investigate the laccase aggregates, SFM micrographs of some aggregates were recorded (Fig. 3). The radius of the particular spot shown in Fig. 3A, B is approximately 7 µm and the height is 1.8 µm. As discussed above, these height variations are not sufficient to cause the current variations in SG/TC mode investigations at $d \approx 20$ µm. The aggregate is surrounded by a dendritic-like structure that is approximately 100 nm high. At the edges the thickness increases and lies in the range of 150–650 nm. The nature of this dendritic-like structure is unknown at present but is reminiscent of other crystallisation and de-mixing processes that are connected with formation of new solid phases.

After exposing the sample to 1 mM $ABTS^{2-}$ in 0.1 M phosphate buffer (pH 4.8) for 22 h and drying it, the very same aggregate was imaged again (Fig. 3C, D). The lateral dimension of the central aggregate has not been changed significantly compared to Fig. 3A, B. The height of the surrounding dendritic-like structure has significantly been reduced to a few nanometres. Only the edges show a peak height of a few tens to several hundred nanometres indicating that some material has been dissolved during the exposure to the aqueous buffer.

The importance of consideration of topographic information for SECM image interpretation has been emphasised earlier [53] and it is a re-occurring problem for most technical samples. Besides distance-control mechanisms (for an overview see [37]), the usage of combined SFM/CLSM/SECM is a useful tool in this context as it does not only allow for precise positioning of the UME with respect to features on the sample. Previously, combinations of CLSM and SECM have been used to characterise diffusion layers in front of microelectrodes using fluorescent dyes [54–57]. In this study, a combined CLSM/SECM setup has been used to generate high quality optical micrographs of the sample to relocate specific features in laccase–silicate films and to precisely position the UME above areas of interest. It was thus possible to obtain images of identical surface regions by means of complementing microscopic techniques (CLSM, SFM, SECM, Fig. 4). The laccase aggregate has been identified using CLSM. This is advantageous because optical microscopy allows to screen large regions on the sample rapidly and then

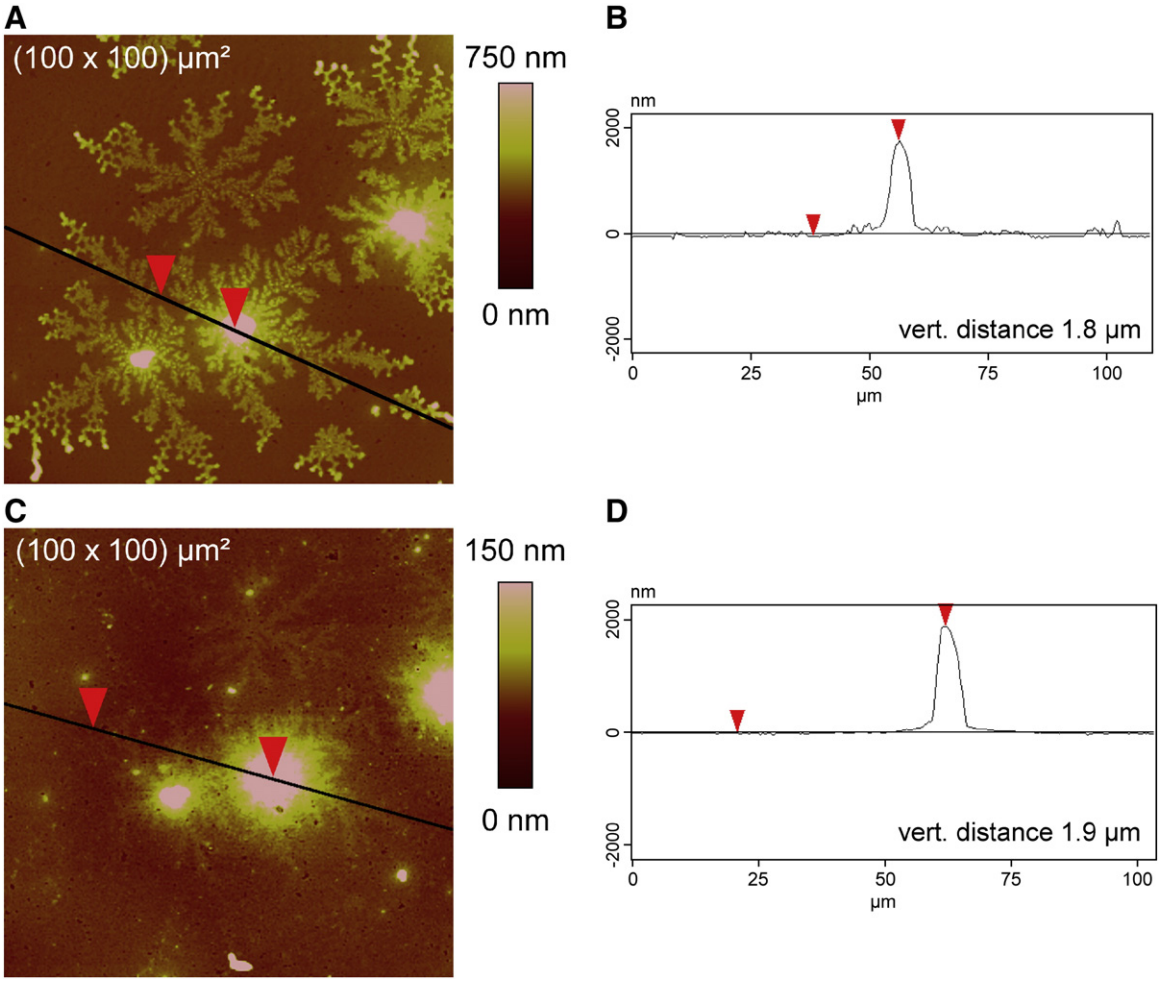

Fig. 3. SFM micrographs of a laccase aggregate. A) False colour representation of the topography of the aggregate of a freshly prepared sample; B) cross section along the black line as in (A); C) false colour representation of the topography of the same aggregate after 22 h exposure to 1 mM $ABTS^{2-}$ in 0.1 M phosphate buffer (pH 4.8); D) cross section as indicated in part (C). Note the different colour scales in (A) and (B). (For interpretation of the references to colour in this figure legend, the reader is referred to the web version of this article.)

to increase magnifications for a more detailed inspection. CLSM measurements allow in addition the reconstruction of topographic information from recorded image stacks [58,59]. As an example, the reconstructed topography of the spot in Fig. 4B is shown in the supporting information. However, the resolution in vertical axis is limited by the wavelength of the light and – more importantly – by the numerical aperture (NA) of the objective used. In the particular experiment that led to Fig. 4B, an objective with a large working distance and suitable for imaging through microscope slides with a thickness of 1 mm had to be used (e.g. HC PL FLUOTAR 10× objective, NA = 0.3). In this case, the nominal resolution in z direction is 4.77 µm. This is too large to make a detailed topographic analysis of features that had been seen in SFM images of laccase–silicate films (Fig. 3). In order to achieve higher resolution, it is important to be able to characterise the very same region on the sample additionally using either SFM or CLSM with an objective with higher numerical aperture (e.g. 50× objective, NA = 0.8, nominal z resolution = 0.549 µm). Typically such objectives cannot image through objective slides and it is required to turn the sample upside down and relocate the region of interest. The same holds for SFM images, in which relocation is typically performed by an optical microscope attached to the setup. Due to the high quality of the optical images, this relocation was possible in the present study. The topography was imaged using Tapping Mode™ SFM (Fig. 4A) and the height of the aggregate was determined to be 2.7 µm. A topographic feature of this height cannot be the reason for the features observed in SG/TC SECM images at working distances of 20 µm. In order to verify the catalytic activity of the aggregate studied in Fig. 4, the imaged area was relocated and reflection mode CLSM image (Fig. 4B) and SECM image (Fig. 4C) were recorded. The CLSM image has a high enough resolution to prove the identity of the aggregates investigated by SFM and SECM (see the structure of the dendritic-like phase around the central aggregate) and can be used to position the UME exactly relative to this feature. The SECM image shows the

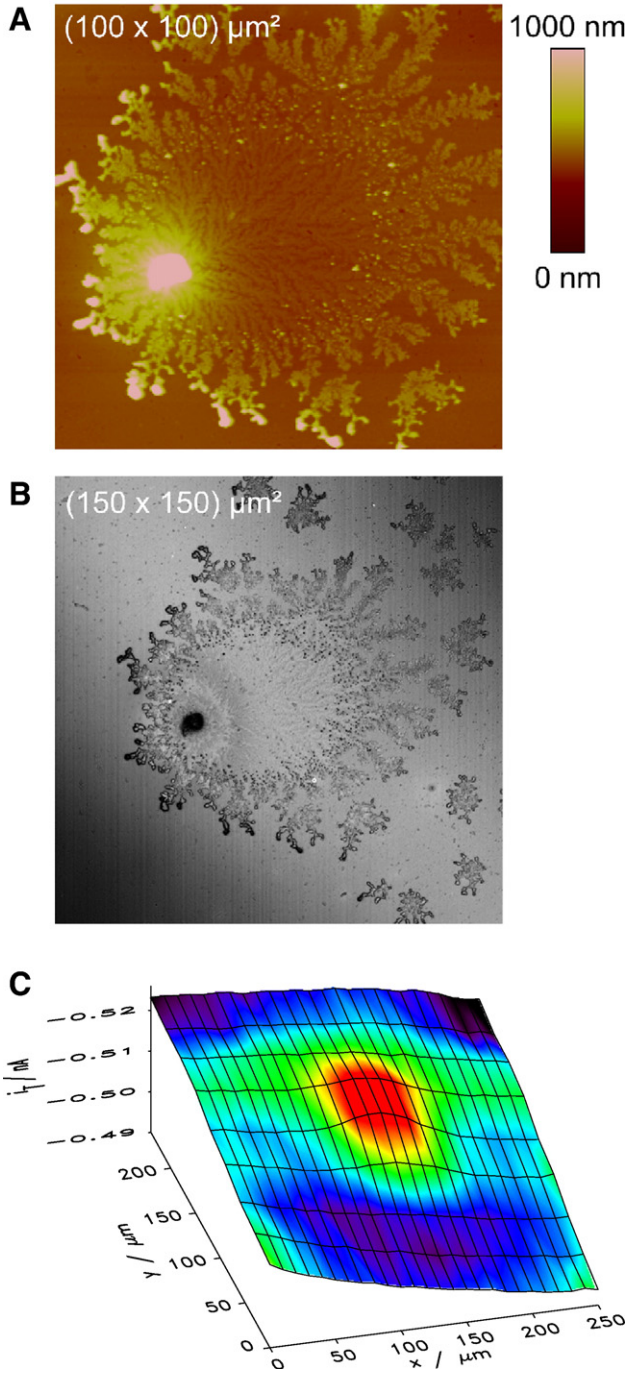

Fig. 4. Subsequent images of one and the same laccase aggregate. A) SFM image, B) CLSM reflection mode image (50× objective), C) SG/TC mode SECM image, E_T=−0.1 V, r_T=5 µm, 1 mM $ABTS^{2-}$+0.1 M phosphate buffer (pH 4.8), v_T=7.7 µm s^{-1}.

enhanced catalytic activity of the particular aggregate under study (Fig. 4C).

4. Conclusion

The embedding of the enzyme laccase in silicate films obtained by a sol–gel process using TMOS as precursor leads to films that show scattered aggregates. The aggregates have been characterised. They extend around 2–4 µm above the film. Around the aggregates a dendritic-like phase is often observed. This phase has a height of 100–500 nm above the film and partially dissolves in aqueous buffers. The exact chemical nature of the dendritic-like phase could not be determined. The central aggregate is most likely laccase. This is concluded from the enhanced catalytic activity that has been determined above such regions using the SG/TC and RC modes of SECM. It has been demonstrated how SFM, CLSM and SECM can be used as complementing techniques to relocate specific features on complicated transparent samples. This opens interesting perspectives for characterisation of a number of technologically important surfaces.

Acknowledgements

The work was funded within a binational exchange programme of the German Academic Exchange Office (DAAD 323-bis PPP Polen) and the Polish Ministry of Science and Higher Education (Research Project PBZ KBN 098/T09/2003).

Appendix A. Supplementary data

Supplementary data associated with this article can be found, in the online version, at doi:10.1016/j.bioelechem.2008.01.010.

References

[1] A.M. Mayer, R.C. Staples, Laccase: new functions for an old enzyme, Phytochemistry 60 (2002) 551–565.
[2] J. Rogalski, A. Leonowicz, Production and application of laccase, in: A. Pandy (Ed.), Concise Encyclopedia of Bioresource Technology, The Haworth Press, Inc., Binghamton, 2004, pp. 533–542.
[3] E.I. Solomon, U.M. Sundaram, T.E. Machonkin, Multicopper oxidases and oxygenases, Chem. Rev. 96 (1996) 2563–2605.
[4] S.A.S.S. Gomes, J.M.F. Nogueira, M.J.F. Rebelo, An amperometric biosensor for polyphenolic compounds in red wine, Biosens. Bioelectron. 20 (2004) 1211–1216.
[5] S. Shleev, P. Persson, G. Shumakovich, Y. Mazhugo, A. Yaropolov, T. Ruzgas, L. Gorton, Laccase-based biosensors for monitoring lignin, Enzyme Microb. Technol. 39 (2006) 835–840.
[6] A.I. Yaropolov, A.N. Kharybin, J. Emneus, G. Marko-Varga, L. Gorton, Flow-injection analysis of phenols at a graphite electrode modified with co-immobilized laccase and tyrosinase, Anal. Chim. Acta 308 (1995) 137–144.
[7] Y. Liu, X. Qu, H. Guo, H. Chen, B. Liu, S. Dong, Facile preparation of amperometric laccase biosensor with multifunction based on the matrix of carbon nanotubes–chitosan composite, Biosens. Bioelectron. 21 (2006) 2195–2201.
[8] D. Quan, Y. Kim, K.B. Yoon, W. Shin, Assembly of laccase over platinum oxide surface and application as an amperometric biosensor, Bull. Korean Chem. Soc. 23 (2002) 385–390.
[9] F. Vianello, A. Cambria, S. Ragusa, M.T. Cambria, L. Zennaro, A. Rigo, A high sensitivity amperometric biosensor using a monomolecular layer of laccase as biorecognition element, Biosens. Bioelectron. 20 (2004) 315–321.
[10] F. Barriere, P. Kavanagh, D. Leech, A laccase–glucose oxidase biofuel cell prototype operating in a physiological buffer, Electrochim. Acta 51 (2006) 5187–5192.
[11] S.C. Barton, H.-H. Kim, G. Binyamin, Y. Zhang, A. Heller, Electroreduction of O_2 to water on the "wired" laccase cathode, J. Phys. Chem. B 105 (2001) 11917–11921.

[12] L. Brunel, J. Denele, K. Servat, K.B. Kokoh, C. Jolivalt, C. Innocent, M. Cretin, M. Rolland, S. Tingry, Oxygen transport through laccase biocathodes for a membrane-less glucose/O_2 biofuel cell, Electrochem. Commun. 9 (2007) 331–336.
[13] T. Chen, S.C. Barton, G. Binyamin, Z. Gao, Y. Zhang, H.-H. Kim, A. Heller, A miniature biofuel cell, J. Am. Chem. Soc. 123 (2001) 8630–8631.
[14] W.E. Farneth, M.B. D'Amore, Encapsulated laccase electrodes for fuel cell cathodes, J. Electroanal. Chem. 581 (2005) 197–205.
[15] W.E. Farneth, B.A. Diner, T.D. Gierke, M.B. D'Amore, Current densities from electrocatalytic oxygen reduction in laccase/ABTS solutions, J. Electroanal. Chem. 581 (2005) 190–196.
[16] J. Fei, A. Basu, F. Xue, G.T.R. Palmore, Two polymerizable derivatives of 2,2'-azino-bis(3-ethylbenzothiazoline-6-sulfonic acid), Org. Lett. 8 (2006) 3–6.
[17] A.M. Kuznetsov, V.A. Bogdanovskaya, M.R. Tarasevich, E.F. Gavrilova, The mechanism of cathode reduction of oxygen in a carbon carrier-laccase system, FEBS Lett. 215 (1987) 219–222.
[18] W. Nogala, E. Rozniecka, I. Zawisza, J. Rogalski, M. Opallo, Immobilization of ABTS — laccase system in silicate based electrode for bioelectrocatalytic reduction of dioxygen, Electrochem. Commun. 8 (2006) 1850–1854.
[19] G.T.R. Palmore, H.-H. Kim, Electro-enzymic reduction of dioxygen to water in the cathode compartment of a biofuel cell, J. Electroanal. Chem. 464 (1999) 110–117.
[20] D. Quan, Y. Kim, W. Shin, Characterization of an amperometric laccase electrode covalently immobilized on platinum surface, J. Electroanal. Chem. 561 (2004) 181–189.
[21] D. Quan, Y. Kim, W. Shin, Sensing characteristics of tyrosinase immobilized and tyrosinase, laccase co-immobilized platinum electrodes, Bull. Korean Chem. Soc. 25 (2004) 1195–1201.
[22] I. Zawisza, J. Rogalski, M. Opallo, Electrocatalytic reduction of dioxygen by redox mediator and laccase immobilized in silicate thin film, J. Electroanal. Chem. 588 (2006) 244–252.
[23] W. Nogala, E. Rozniecka, J. Rogalski, M. Opallo, pH-Sensitive syringaldazine modified carbon ceramic electrode for bioelectrocatalytic dioxygen reduction, J. Electroanal. Chem. 608 (2007) 31–36.
[24] K. Szot, J. Niedziolka, J. Rogalski, F. Marken, M. Opallo, Bioelectrocatalytic dioxygen reduction at hybrid silicate–polyallylamine film with encapsulated laccase, J. Electroanal. Chem. 612 (2008) 1–8.
[25] R.A. Bullen, T.C. Arnot, J.B. Lakeman, F.C. Walsh, Biofuel cells and their development, Biosens. Bioelectron. 21 (2006) 2015–2045.
[26] F. Davis, S.P.J. Higson, Biofuel cells—recent advances and applications, Biosens. Bioelectron. 22 (2007) 1224–1235.
[27] A. Heller, Miniature biofuel cells, Phys. Chem. Chem. Phys. 6 (2004) 209–216.
[28] E. Katz, A.N. Shipway, I. Willner, in: W. Vielstich, H. Gasteiger, A. Lamm (Eds.), Handbook of Fuel Cell Technology, Wiley, New York, 2003.
[29] D. Avnir, T. Coradin, O. Lev, J. Livage, Recent bio-applications of sol–gel materials, J. Mater. Chem. 16 (2006) 1013–1030.
[30] S. Braun, S. Rappoport, R. Zusman, D. Avnir, M. Ottolenghi, Biochemically active sol–gel glasses: the trapping of enzymes, Mater. Lett. 10 (1990) 1–5.
[31] R.A. Simkus, V. Laurinavicius, L. Boguslavsky, T. Skotheim, S.W. Tanenbaum, J.P. Nakas, D.J. Slomczynski, Laccase containing sol–gel based optical biosensors, Anal. Lett. 29 (1996) 1907–1919.
[32] R.C. Engstrom, M. Weber, D.J. Wunder, R. Burgess, S. Winquist, Measurements within diffusion layer using a microelectrode probe, Anal. Chem. 58 (1986) 844–848.
[33] H.-Y. Liu, F.-R.F. Fan, C.W. Lin, A.J. Bard, Scanning electrochemical and tunneling ultramicroelectrode microscope for high-resolution examination of electrode surfaces in solution, J. Am. Chem. Soc. 108 (1986) 3838–3839.
[34] A.J. Bard, F.-R.F. Fan, J. Kwak, O. Lev, Scanning electrochemical microscopy. Introduction and principles, Anal. Chem. 61 (1989) 132–138.
[35] D.T. Pierce, P.R. Unwin, A.J. Bard, Scanning electrochemical microscopy. 17. Studies of enzyme — mediator kinetics for membrane- and surface-immobilized glucose oxidase, Anal. Chem. 64 (1992) 1795–1804.
[36] B.R. Horrocks, G. Wittstock, Biological systems, in: A.J. Bard, M.V. Mirkin (Eds.), Scanning Electrochemical Microscopy, Marcel Dekker, New York, Basel, 2001, pp. 445–519.
[37] G. Wittstock, M. Burchardt, S.E. Pust, Y. Shen, C. Zhao, Scanning electrochemical microscopy for direct imaging of reaction rates, Angew. Chem. Int. Ed. 46 (2007) 1584–1617.
[38] G. Wittstock, W. Schuhmann, Formation and imaging of microscopic enzymatically active spots on an alkanethiolate-covered gold electrode by scanning electrochemical microscopy, Anal. Chem. 69 (1997) 5059–5066.
[39] H. Shiku, T. Matsue, Microamperometric sensing of localized biomolecules, in: W. H. Baltes, Göpel, J. Hesse (Eds.), Sensors Update Bd.6. WILEY-VCH, Weinheim, 2000.
[40] J.L. Fernandez, N. Mano, A. Heller, A.J. Bard, Analytical methods: optimization of "wired" enzyme O_2-electroreduction catalyst compositions by scanning electrochemical microscopy, Angew. Chem. Int. Ed. 43 (2004) 6355–6357.
[41] K. Karnicka, K. Eckhard, D.A. Guschin, L. Stoica, P.J. Kulesza, W. Schuhmann, Visualisation of the local bio-electrocatalytic activity in biofuel cell cathodes by means of redox competition scanning electrochemical microscopy (RC-SECM), Electrochem. Commun. 9 (2007) 1998–2002.
[42] K. Eckhard, X. Chen, F. Turcu, W. Schuhmann, Redox competition mode of scanning electrochemical microscopy (RC-SECM) for visualisation of local catalytic activity, Phys. Chem. Chem. Phys. 8 (2006) 5359–5365.
[43] J. Rogalski, A. Dawidowicz, E. Jozwik, A. Leonowicz, Immobilization of laccase from Cerrena unicolor on controlled porosity glass, J. Mol. Catal. B: Enzym. 6 (1999) 29–39.
[44] G. Janusz, Comparative studies of fungal laccases, PhD thesis, Maria Curie-Sklodowska University, Lublin, 2005.
[45] A. Leonowicz, K. Grzywnowicz, Quantitative estimation of laccase forms in some white-rot fungi using syringaldazine as a substrate, Enzyme Microb. Technol. 3 (1981) 55–58.
[46] M.M. Bradford, A rapid and sensitive method for the quantitation of microgram quantities of protein utilizing the principle of protein-dye binding, Anal. Biochem. 72 (1976) 248–254.
[47] C. Nunes Kirchner, K.H. Hallmeier, R. Szargan, T. Raschke, C. Radehaus, G. Wittstock, Evaluation of thin film titanium nitride electrodes for electroanalytical applications, Electroanalysis 19 (2007) 1023–1031.
[48] C. Nunes Kirchner, S. Szunerits, G. Wittstock, Scanning electrochemical microscopy (SECM) based detection of oligonucleotide hybridization and simultaneous determination of the surface concentration of immobilized oligonucleotides on gold, Electroanalysis 19 (2007) 1258–1267.
[49] G. Wittstock, T. Asmus, T. Wilhelm, Investigation of ion-bombarded conducting polymer films by scanning electrochemical microscopy (SECM), Fresenius J. Anal. Chem. 367 (2000) 346–351.
[50] C. Kranz, M. Ludwig, H.E. Gaub, W. Schuhmann, Lateral deposition of polypyrrole lines by means of the scanning electrochemical microscope, Adv. Mater. 7 (1995) 38–40.
[51] Y. Saito, A theoretical study on the diffusion current at the stationary electrodes of circular and narrow band types, Rev. Polarogr. 15 (1968) 177–187.
[52] E.R. Scott, H.S. White, J.B. Phipps, Ionotophoretic transport through porous membranes using scanning electrochemical microscopy: application to in vitro studies of ion fluxes through skin, Anal. Chem. 65 (1993) 1537–1545.
[53] G. Wittstock, H. Emons, M. Kummer, J.R. Kirchhoff, W.R. Heineman, Application of scanning electrochemical microscopy and scanning electron microscopy for the characterization of carbon-spray modified electrodes, Fresenius J. Anal. Chem. 348 (1994) 712–718.
[54] F.-M. Boldt, J. Heinze, M. Diez, J. Petersen, M. Boersch, Real-time pH microscopy down to the molecular level by combined scanning electrochemical microscopy/single-molecule fluorescence spectroscopy, Anal. Chem. 76 (2004) 3473–3481.
[55] N.C. Rudd, S. Cannan, E. Bitziou, I. Ciani, A.L. Whitworth, P.R. Unwin, Fluorescence confocal laser scanning microscopy as a probe of ph gradients in electrode reactions and surface activity, Anal. Chem. 77 (2005) 6205–6217.

[56] A.L. Barker, P.R. Unwin, J.W. Gardner, H. Rieley, A multi-electrode probe for parallel imaging in scanning electrochemical microscopy, Electrochem. Commun. 6 (2004) 91–97.
[57] S. Cannan, I.D. Macklam, P.R. Unwin, Three-dimensional imaging of proton gradients at microelectrode surfaces using confocal laser scanning microscopy, Electrochem. Commun. 4 (2002) 886–892.
[58] D.K. Hamilton, T. Wilson, Three-dimensional surface measurement using the confocal scanning microscope, Appl. Phys. B 27 (1982) 211–213.
[59] S. Wessel, S. Pagel, M. Ritter, H. Hohenberg, R. Wepf, Topographic measurements of real structures in reflection confocal laser scanning microscope (CLSM), Microsc. Microanal. 9 (2003) 162–163.